TABLE I. Solutions of the bootstrap equations for $N=8$. M_{K^*} is the unit of mass. The coefficients which multiply the g's exhibited here to give the actual g's are given in the text.

	$M_{\rho\pm}$	$M_{\rho 0}$	M_{ϕ}	$(g_{\phi K^*K^*})^2$	$(g_{\rho\pm K^*K^*})^2$	$(g_{\rho 0 K^*K^*})^2$	$(g_{\rho\rho\rho})^2$
SU_3 symmetric:							
$x=2$ or $x=\infty$	1	1	1	1	1	1	1
Charge-independent							
$x=\infty$	1.55	1.55	0.91	1.49	0.66	0.66	0.16
$x=2$	1.33	1.33	0.93	1.37	0.83	0.83	0.26
Charge-dependent:							
$x=\infty$	1.63	1.41	0.90	1.46	0.47	1.01	0.13
$x=2$	1.47	1.19	0.93	1.37	0.47	1.49	0.24

so that the ρ is mainly a $(\bar{K}^*K^*)$ bound state. One can see from the second and third equations of Fig. 4(a) that a difference between $g_{\rho\pm K^*K^*}$ and $g_{\rho 0 K^*K^*}$ can regenerate in such a case and the minus signs in these equations and in those for N_0 and $N_\pm$ allow a reciprocal amplification of mass and coupling-constant differences. This presumably would not happen if $M_\rho<M_{K^*}<M_\phi$, since then ρ would be mostly $(\rho\rho)$ and the first terms of the equations would dominate, leading to stability as for $N=3$.

PHYSICAL REVIEW VOLUME 138, NUMBER 3B 10 MAY 1965

Proton-Proton Scattering at 1.48 BeV*

A. M. EISNER,† E. L. HART, R. I. LOUTTIT, AND T. W. MORRIS
Brookhaven National Laboratory, Upton, New York
(Received 31 December 1964)

A sample of 2657 proton-proton scattering events at 1.48 BeV has been analyzed. The elastic cross section is 19.86 mb, and the elastic scattering is consistent with a simple opaque-disk optical model with $R=0.91$ F and $1\text{-}a=0.864$. The dominant feature of the inelastic scattering is the production of the (3/2, 3/2) isobar. The reaction $p+p\rightarrow p+n+\pi^+$ is interpreted satisfactorily in terms of the one-pion-exchange model.

INTRODUCTION

IN the last four or five years, a number of experimenters have investigated proton-proton interactions in the 1–3 BeV range utilizing electronic counters[1–3] or the liquid-hydrogen bubble chamber.[4–8] As a continuation of this investigation the BNL twenty-inch bubble chamber was exposed to a beam of 1.48-BeV protons from the Cosmotron. This paper reports the results from the analysis of the 2657 measured events. Detailed results are given only for elastic and $pn+$ events, because only in those cases were there sufficient events to make results statistically meaningful.

In previous experiments, the simple optical model of a purely absorbing disk[9] has been found to explain satisfactorily the angular distribution of elastic events over a wide range of scattering angles. This model is therefore used to analyze the elastic events and to correct for scanning biases due to the difficulty of observing small-angle scatters.

Momentum and effective-mass distributions for $pn+$ events are compared with the predictions of the Stern-

* Work performed under the auspices of the U. S. Atomic Energy Commission.

† Present address: Department of Physics, Harvard University, Cambridge, Massachusetts.

[1] M. J. Longo and B. J. Moyer, Phys. Rev. **125**, 701 (1962).

[2] T. Fujii, G. B. Chadwick, G. B. Collins, P. J. Duke, N. C. Hien, M. A. R. Kemp, and F. Turkot, Phys. Rev. **128**, 1836 (1962); G. B. Chadwick, G. B. Collins, P. J. Duke, T. Fujii, N. C. Hien, M. A. R. Kemp, and F. Turkot, *ibid.* 1823 (1962).

[3] F. F. Chen, C. P. Leavitt, and A. M. Shapiro, Phys. Rev. **103**, 211 (1956); B. Cork, W. A. Wenzel, and C. W. Causey, *ibid.* **107**, 859 (1957); M. J. Longo, J. A. Helland, W. N. Hess, B. J. Moyer, and V. Perez-Mendez, Phys. Rev. Letters **3**, 568 (1959); M. J. Longo, thesis, University of California Radiation Laboratory Report UCRL-9497, 1961 (unpublished); G. Von Dardel, D. H. Frisch, R. Mermod, R. H. Milburn, P. A. Piroue *et al.*, Phys. Rev. Letters **5**, 333 (1960).

[4] G. A. Smith, H. Courant, E. C. Fowler, H. Kraybill, J. Sandweiss, and H. Taft, Phys. Rev. **123**, 2160 (1961); G. A. Smith, H. Courant, E. C. Fowler, H. Kraybill, J. Sandweiss, and H. Taft, Phys. Rev. Letters **5**, 571 (1960).

[5] W. J. Fickinger, E. Pickup, D. K. Robinson, and E. O. Salant, Phys. Rev. Letters **7**, 196 (1961).

[6] W. J. Fickinger, E. Pickup, D. K. Robinson, and E. O. Salant, Phys. Rev. **125**, 2082, 2091 (1962).

[7] E. L. Hart, R. I. Louttit, D. Luers, T. W. Morris, W. J. Willis, and S. S. Yamamoto, Phys. Rev. **126**, 747 (1962).

[8] D. V. Bugg, A. J. Oxley, J. A. Zoll, J. G. Rushbrooke, V. E. Barnes *et al.*, Phys. Rev. **133**, B1017 (1964).

[9] S. Fernbach, R. Serber, and T. B. Taylor, Phys. Rev. **75**, 1352 (1949).

heimer and Lindenbaum isobar model.[10,11] This model assumes that $pn+$ production takes place via the excitation of one nucleon to an $I=3/2$ or $I=1/2$ isobar state, which subsequently decays to a nucleon and a pion. However, in order to predict angular distributions and absolute values of cross sections, it is necessary to choose a specific mechanism for the interaction. The one-pion-exchange model is such a mechanism; it assumes that single-pion production proceeds via the scattering, by one nucleon, of a virtual pion emitted by the other nucleon. The experimental results are compared with several predictions of this model.

EXPERIMENTAL PROCEDURE

The external beam of the Cosmotron was focused on a 5-cm-thick beryllium target. The protons were diffraction-scattered by the target at 15° and deflected by several steering magnets into the bubble chamber. The energy of the incident beam was 1.48 BeV, and the total path length in air after the target was 29 m. The combined dispersion of the magnets was calculated to give a momentum spread of 1.7 MeV/c across the 5-cm-wide collimator placed in front of the chamber.

Four thousand pictures were taken with about 15 beam tracks per picture. Events were accepted only within a restricted fiducial volume. Measurements were made using digitized projectors, and the data processed with standard computer programs, including the GUTS kinematics-fitting routine.

The events were interpreted using the results of the kinematics program as well as visual estimates of ionization. Interpretations involving one-constraint fits (one neutral particle) were required to have a $\chi^2 \leq 4$. Four-constraint fits (no neutrals) were required to have a $\chi^2 \leq 25$, with the further requirement that elastic events be coplanar within three standard deviations. Events with two neutral particles were identified by the missing mass and by the absence of acceptable fits. In all cases, the estimated ionization was required to be consistent with that predicted by the interpretation. Nearly every event was unambiguously classified according to the final states listed in Table I.

TABLE I. Partial cross sections.

Final state	Events observed	Corrected partial cross section (mb)
pp	1072	$19.86_{-0.64}{}^{+0.73}$
$pn+$	1048	$17.22_{-0.57}{}^{+0.66}$
$pp0$	242	$3.98_{-0.26}{}^{+0.27}$
$d+$	8	0.13 ± 0.05
$d+0$	26	0.43 ± 0.08
$++nn$	15	0.25 ± 0.06
$pp00$	25	0.41 ± 0.08
$p+n0$	144	2.37 ± 0.20
$pp+-$	58	1.22 ± 0.14
$pp+-0$	1	0.02 ± 0.02
$pp+-n$	1	0.02 ± 0.02

[10] S. J. Lindenbaum and R. M. Sternheimer, Phys. Rev. **105**, 1874 (1957).
[11] R. M. Sternheimer and S. J. Lindenbaum, Phys. Rev. **123**, 333 (1961).

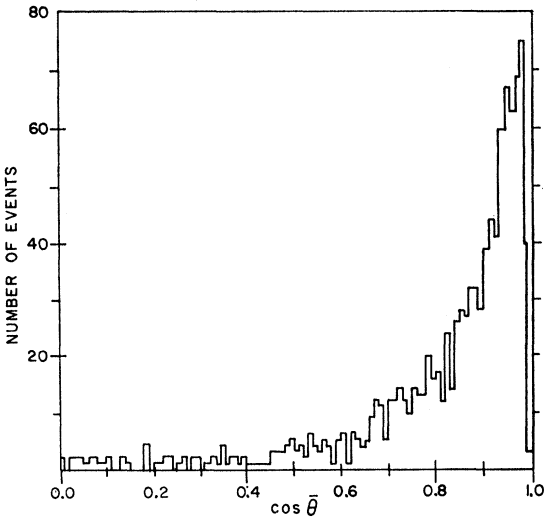

FIG. 1. Elastic center-of-mass angular distribution.

The final value of the beam momentum was obtained by varying it in a sample of elastic events before kinematic fitting. The momentum which gave the lowest average χ^2 for the sample was accepted. This value agreed with the value obtained by measuring an independent sample of long beam tracks. The beam momentum thus obtained was 2.23 BeV/c, with a spread (full width at half-height) of 0.12 BeV/c.

ELASTIC SCATTERING

Scanning biases against observing small-angle elastic scattering or events with steep recoil paths necessitate making corrections to the number of elastic events detected. Figure 1 shows the distribution of the c.m. scattering angle; it is evident that the small-angle losses are significant for $\cos\theta_{\text{c.m.}} \geq 0.98$. This graph does not include 12 events added to correct for azimuthal losses in the region $0.94 \leq \cos\theta_{\text{c.m.}} < 0.98$. These were events missed because the plane of the event lay in or near a plane passing through the camera lens. A visual extrapolation of the histogram in Fig. 1 to $\cos\theta=1$ indicates that between 120 and 142 events should be added to the 1054 measured.

To obtain a more precise estimate, the data were fitted to the simple optical model of a purely absorbing disk of radius R and transmitted amplitude a. If $\hbar k$ is the c.m. momentum of the incident proton, then the momentum transfer is given by

$$\Delta = 2\hbar k \sin(\tfrac{1}{2}\theta_{\text{c.m.}}).$$

Then the simple optical model[9] predicts an elastic

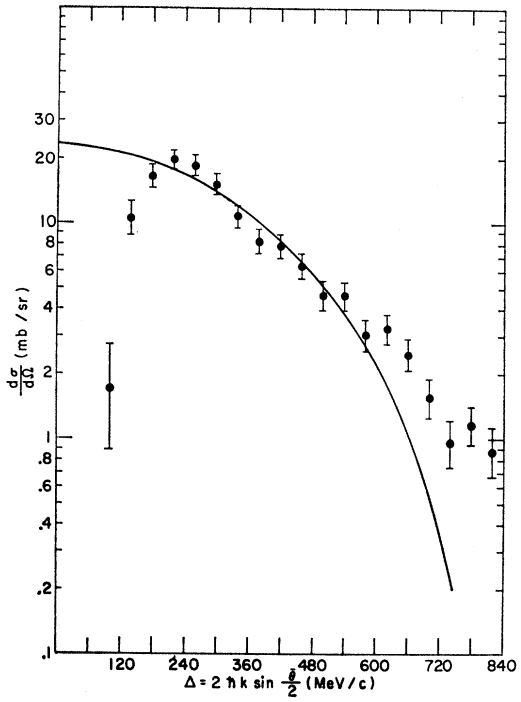

FIG. 2. Elastic differential cross section versus momentum transfer. The curve represents a least-squares fit to an opaque-disk optical-model prediction in the region $200<\Delta<600$ MeV/c.

differential cross section given by

$$\frac{1}{k^2}\frac{d\sigma}{d\Omega}=R^2(1-a)^2\left[\frac{J_1(\Delta R/\hbar)}{\Delta/\hbar}\right]^2$$
$$=\frac{\sigma_e}{\pi}\left[\frac{J_1(\Delta R/\hbar)}{\Delta/\hbar}\right]^2.$$

For $\Delta<200$ MeV/c, events are lost due to scanning bias; for $\Delta>600$ MeV/c (corresponding to $\theta_{\text{c.m.}}\approx 42°$), the simple optical model is no longer expected to be valid. Therefore, a least-squares fit of the number of events as a function of Δ was made only for Δ between these values. The best fit, shown in Fig. 2 with the experimental values, is for $R=0.91$ F and $1-a\approx 0.864$, the latter derived using the cross sections of the next section. These results are consistent with the earlier results from 0.35 to 6.15 BeV, as summarized by Fujii *et al.*[2] in their Table II. This method leads to an addition of 135 events to correct for the scanning loss at $\cos\theta>0.98$. The fit is adequate, giving a $\chi^2=12.49$ with 9 degrees of freedom. Moreover, any errors introduced by this procedure in the partial cross sections are small compared with the statistical errors and the errors arising from the uncertainty in the value of the total cross section.

PARTIAL CROSS SECTIONS

The value of the total cross section used to obtain the partial cross sections was taken to be $45.9_{-0.5}^{+1.0}$ mb, from the interpolated curve of Longo and Moyer.[1] The resulting values of the partial cross sections are given in Table I, after taking into account the corrected value of the number of elastic events. The errors are largely statistical, but also include a contribution due to the uncertainty in σ_{total}.

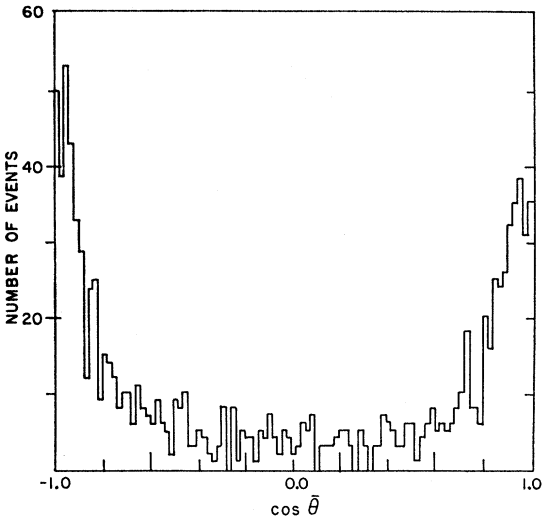

FIG. 3. Center-of-mass angular distribution of protons from $pn+$ events.

A possible additional scanning bias is apparent in the c.m. angular distribution of protons from $pn+$ events, as shown in Fig. 3. The region $-1.0\leqq\cos\theta<-0.4$ has nearly 70 more events than the region $0.4<\cos\theta\leq 1.0$. This amounts to a difference of about three standard deviations. Similar asymmetries have occurred in previous bubble-chamber experiments, amounting to about two standard deviations.[4,6,8] It seems likely that this effect is due to a genuine bias, which may be caused by misidentification of events; however, we consider it more probable that some events with fast, forward-going protons were missed in scanning. If this explanation is true, there may also have been losses for events other than $pn+$. Thus the numbers in Table I

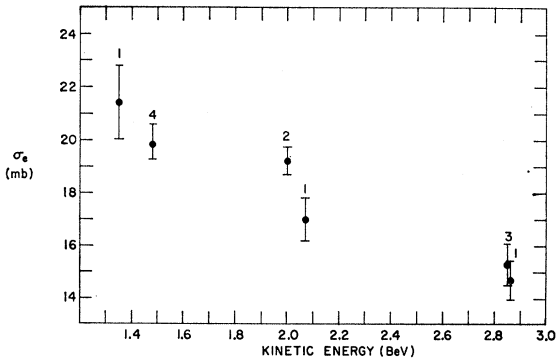

FIG. 4. The elastic cross section at various energies. The points labeled 1 are from Ref. 2; point 2, Ref. 6; point 3, Ref. 4; point 4, this experiment.

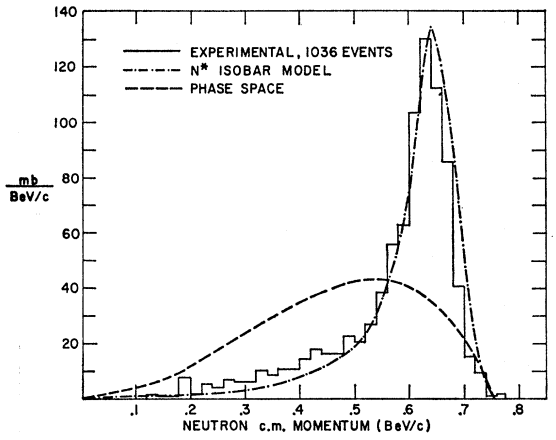

FIG. 5. Center-of-mass momentum distribution of neutrons from $pn+$ events, including predictions of phase space and the isobar model.

may be subject to a small systematic error ($\approx 3\%$ if most of the losses are in $pn+$ events).

The elastic cross section is directly compared with earlier results at other energies as summarized by Fujii *et al.* The results are plotted in Fig. 4. Our result is consistent with the others.

Among the inelastic events, statistically meaningful results can be obtained only for the reaction

$$p+p \rightarrow p+n+\pi^+.$$

Also, various theoretical predictions take their simplest form, and will be easiest to test, for this case. Therefore the rest of this paper will be concerned with this reaction.

$pn+$ EVENTS

A. Isobar Model

Sternheimer and Lindenbaum's original isobar model[10] yields momentum and effective-mass distributions by assuming that the reaction $pp \rightarrow pn+$ proceeds through the excitation of the $(\frac{3}{2},\frac{3}{2})$ $p\pi^+$ resonance, N_1*. An extended version of this model[11] includes the effects of the first $I=\frac{1}{2}$ resonances, N_2*, at $Q_{\pi p}\approx 430$ and 600 MeV. The relative importance of the $I=\frac{1}{2}$ and $I=\frac{3}{2}$ effects may be measured by the $pn+/pp0$ branching ratio. Isotopic-spin arguments show that for pure $I=\frac{3}{2}$ this ratio will equal 5, and that in general (assuming the model of scattering via an isobar state),

$$\sigma_{pn+}=\tfrac{5}{6}\sigma(N_1^*)+\tfrac{2}{3}\sigma(N_{2,S}^*),$$
$$\sigma_{pp0}=\tfrac{1}{6}\sigma(N_1^*)+\tfrac{1}{3}\sigma(N_{2,S}^*),$$

where N_2* is the $Q=430$ isobar, the only $I=\frac{1}{2}$ isobar we have the energy to produce, and $\sigma(N_{2,S}^*)$ is the cross section for its production and subsequent decay into a single pion. (See Sternheimer and Lindenbaum's Table III.[11])

The ratios at several energies are summarized in Table II. It is seen that $\sigma_{pn+}/\sigma_{pp0}$ increases with decreasing energy and reaches a value of 5 at 0.97 BeV, which is below the N_2* production threshold (1.32 BeV). At our energy, N_2* contributes only a small fraction of

TABLE II. Ratios of partial cross sections at different energies.

Energy (BeV)	$\sigma_{pn+}/\sigma_{pp0}$	$\sigma(N_1^*)/\sigma(N_{2,S}^*)$
0.97	4.95±0.45	...
1.48	4.33±0.31	7.0
2.02	4.17±0.25	5.2
2.85	3.94±0.48	3.7

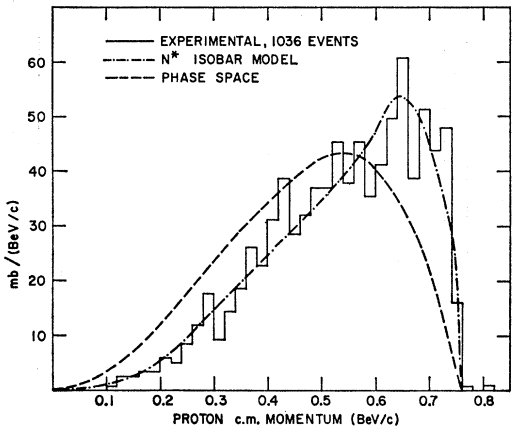

FIG. 6. Proton center-of-mass momentum distribution from $pn+$ events.

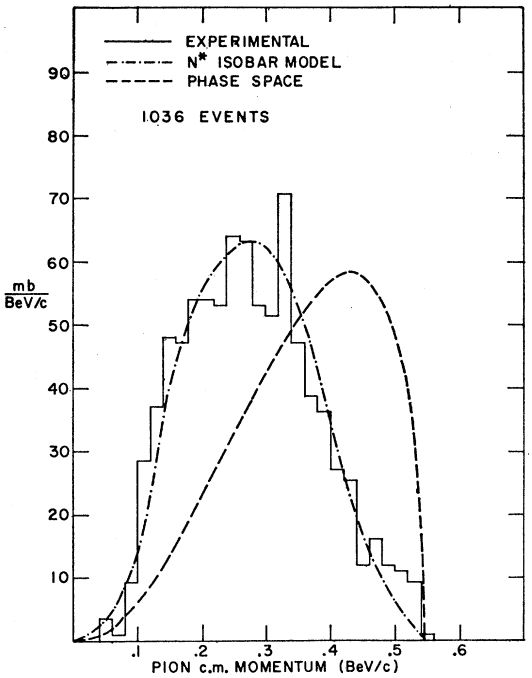

FIG. 7. Pion center-of-mass momentum distribution from $pn+$ events.

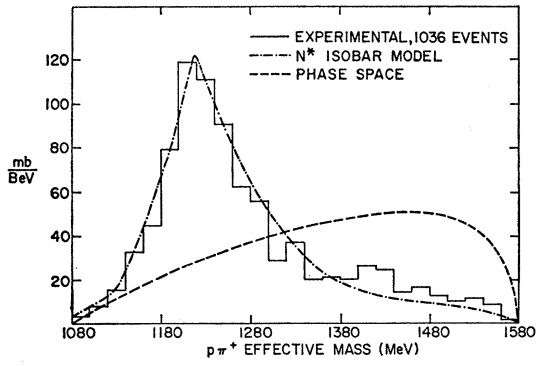

FIG. 8. Effective-mass distribution of pions and protons from $pn+$ events. Phase-space and isobar-model predictions are shown.

events and will be ignored for the rest of this paper. Even at 2.02 BeV the momentum distributions predicted by the extended isobar model differ from those of the single-isobar model by less than the statistical errors of the experimental results.

Figures 5, 6, and 7 show the experimental c.m. momentum distributions for the neutrons, protons, and pions, respectively, in $pn+$ events. These are compared with the predicted isobar model and phase-space (statistical-model) curves normalized to the same area. Figure 8 shows the experimental and two theoretical distributions of the $p\pi^+$ effective mass w (w is defined as the total energy of the proton and pion in the isobar rest system). In all cases the isobar model gives reasonably good agreement with the experiment.

One of the premises of the isobar model is that its decay is isotropic in its own rest frame. The isobar decay angle δ is defined as the angle the pion makes in the isobar frame with the direction in which the isobar is moving in the c.m. system. Figures 9 and 10 show the distribution of δ for all events and for events in the isobar peak (1160 MeV$\leq w \leq$1300 MeV), respectively. Neither distribution is consistent with isotropy, with χ^2 probabilities less than 0.01.

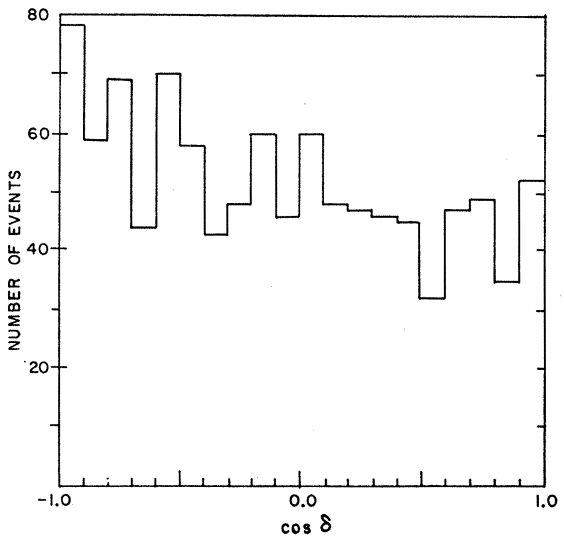

FIG. 9. Isobar-decay angular distribution for all $pn+$ events; the angle which the pion makes in the isobar frame with the direction in which the isobar is moving in the c.m. system.

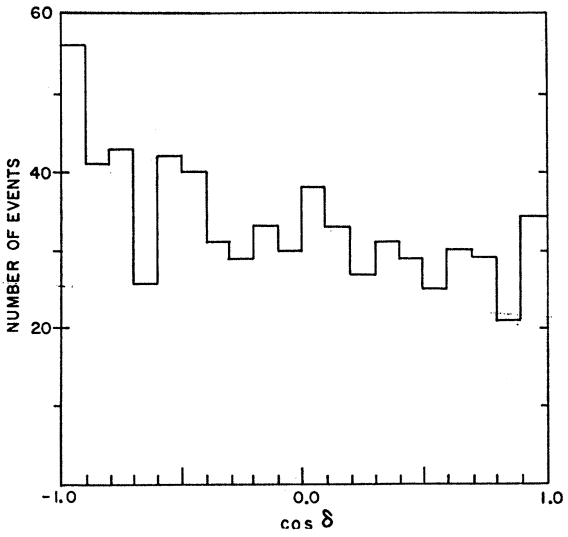

FIG. 10. Isobar-decay angular distribution for events in the isobar peak only; that is, in the effective-mass range 1160–1300 MeV.

B. One-Pion Exchange

Figure 11 shows the c.m. angular distribution of neutrons from $pn+$ events. The sharp forward-backward peaking indicates that the interaction is largely peripheral. An explanation of such peripheral collisions has been proposed in the one-pion-exchange model (OPEM). It may be shown that, if Δ^2 is the square of the invariant four-momentum transfer

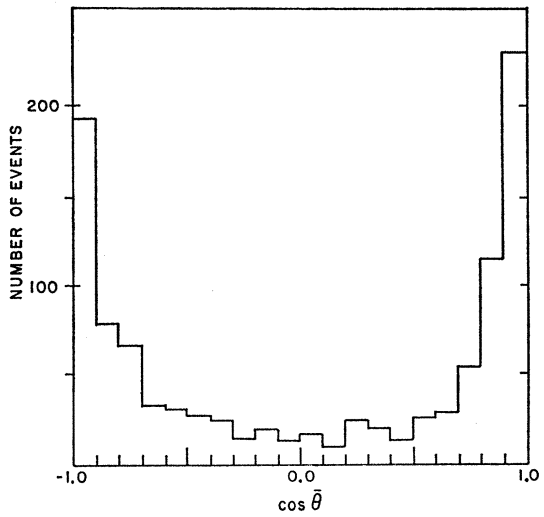

FIG. 11. Center-of-mass angular distribution of neutrons from $pn+$ events.

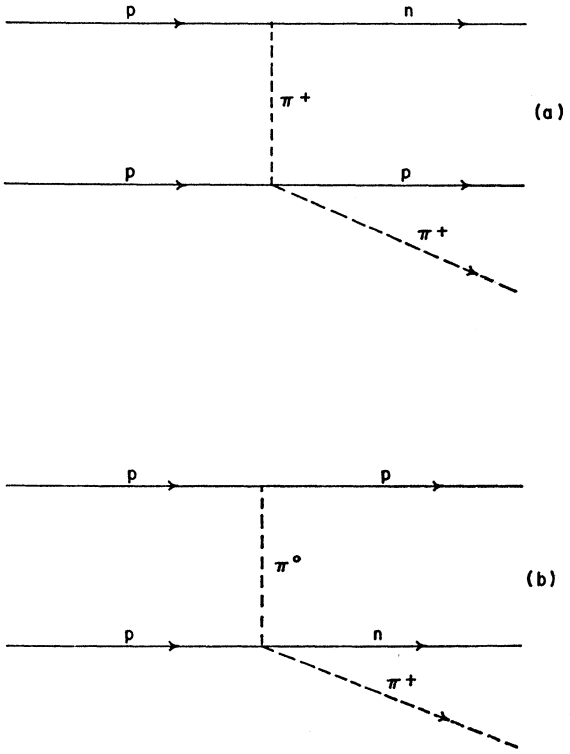

FIG. 12. Feynman diagrams for the one-pion-exchange process.

between incident proton and recoil neutron, then the scattering amplitude has a pole at $\Delta^2=-m_\pi{}^2$.[12] The OPEM assumes that this one-pion pole dominates the interaction in the physical region ($\Delta^2\geq 0$), at least for small Δ^2. The two possible OPEM Feynman diagrams for $pn+$ events are shown in Fig. 12. In each, a virtual

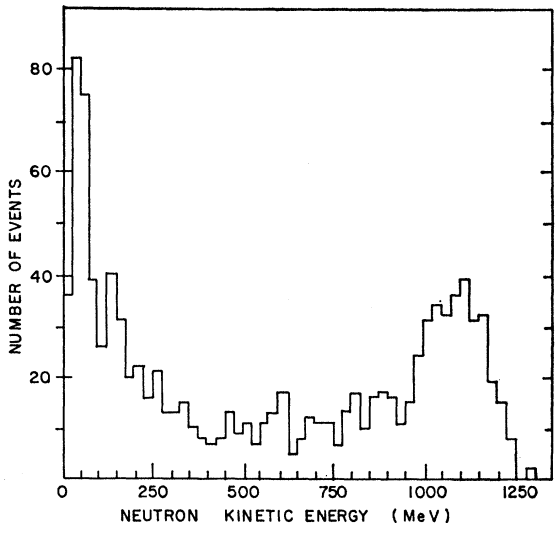

FIG. 13. Laboratory kinetic-energy distribution of neutrons from $pn+$ events.

[12] G. F. Chew and F. E. Low, Phys. Rev. **113**, 1640 (1959).

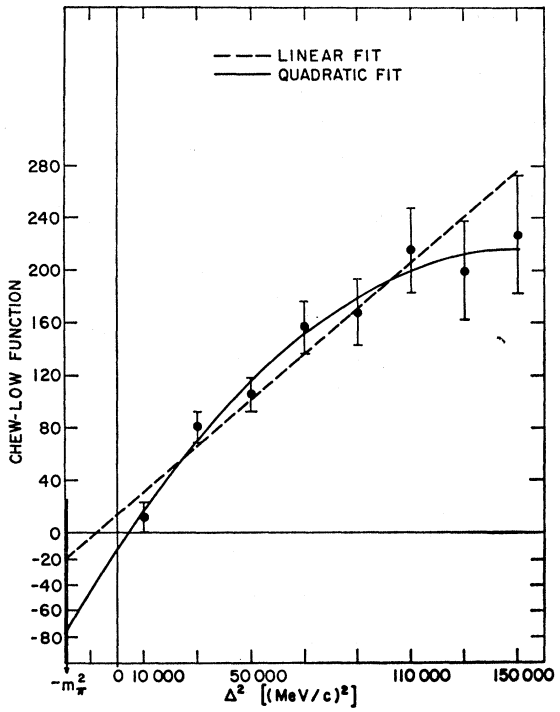

FIG. 14. Plot of the Chew-Low function for events in the isobar peak, including linear and quadratic extrapolations to the one-pion pole.

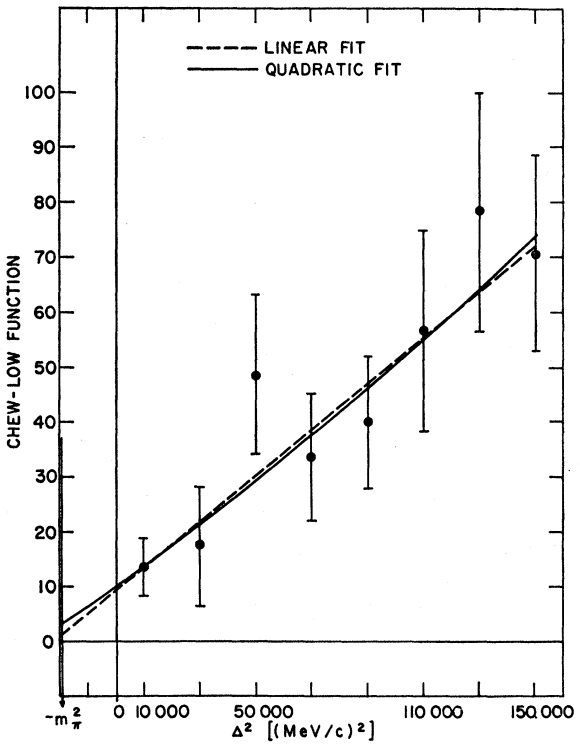

FIG. 15. The Chew-Low function plotted for events outside the isobar peak.

pion is exchanged between the nucleons and scattered off the nucleon at the lower vertex. Isotopic-spin arguments show that for events in or near the isobar peak, the process of Fig. 12(b) should occur only about $\frac{1}{9}$ as often as that of Fig. 12(a) and may be neglected for the purposes of a rough comparison with theory, at least in the isobar peak.

The OPEM analysis must take place in the rest frame of the target proton, that is, the frame of the initial proton at the lower vertex in Fig. 12(a). In order to specify which initial proton is the target, we utilize the frame (either the lab system or the rest frame of the beam proton) in which the collision is more peripheral, i.e., in which Δ^2 is smaller. Figure 13 shows the laboratory kinetic-energy distribution of the neutrons. The selection process for the Δ^2 is equivalent to choosing the frame in which the neutron kinetic energy is greater.

Chew and Low[12] have shown that the residue of $\partial^2\sigma/\partial w^2\partial p^2$ at the one-pion pole in the S matrix is proportional to the π^+p scattering cross section at the same c.m. total energy w, where

$$p^2=(m_n/m_p)[\Delta^2+(m_n-m_p)^2]\approx\Delta^2.$$

They find that

$$\sigma_{\pi^+p}(w)=-\frac{F(w^2,p_0^2)}{0.16},$$

where

$$F(w^2,p^2)=2\pi\left(\frac{m_p}{m_n}\right)^2 \times\frac{q_{1L}^2(p^2-p_0^2)^2}{[\frac{1}{4}w^4-\frac{1}{2}w^2(m_p^2+m_\pi^2)+\frac{1}{4}(m_p^2-m_\pi^2)^2]^{1/2}}\frac{\partial^2\sigma}{\partial w^2\partial p^2}.$$

Here q_{1L} is the lab momentum of the incoming proton, and

$$p_0^2=-\frac{m_n}{m_p}[m_\pi^2-(m_n-m_p)^2].$$

The value of the function at the pole $F(w^2,p_0^2)$ is obtained by extrapolation of F (at fixed w^2) from low physical values of Δ^2 to the pole.

Figure 14 shows linear and quadratic extrapolations for all events in the isobar peak (1160 MeV$<w<$1300 MeV) and Fig. 15 shows similar curves for events not in the peak. Figure 14 gives the π^+p cross section averaged over the peak region: 127±76 mb and 475 mb for the linear and quadratic fits, respectively. The measured average σ_{π^+p} in the peak region is about 140 mb.[13] For events not in the peak, the extrapolation gives a cross section very close to zero. Unfortunately the sample of 1036 $pn+$ events analyzed was not large enough to define the points sufficiently well to indicate what sort of extrapolation should be performed. Our results are similar to those obtained at 2.02 BeV[6] and 2.85 BeV.[4] A simple averaging of the results of the three experiments yields $\sigma_{\pi^+p}=115$ mb for the linear extrapolation in the peak region.

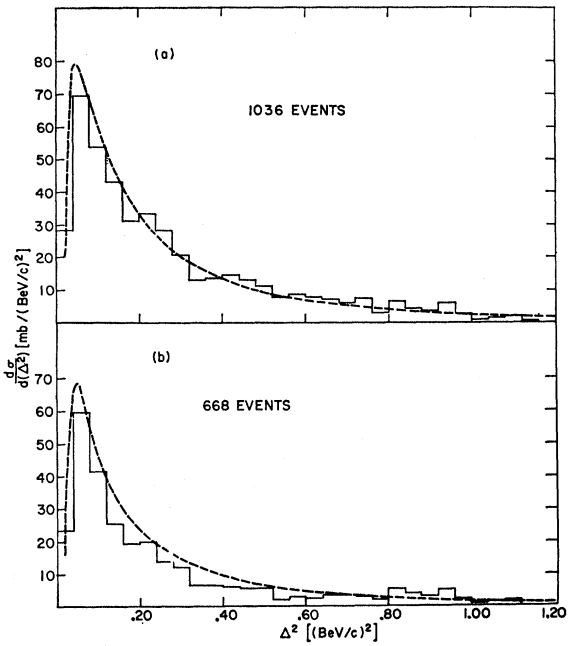

FIG. 16. Distribution of the square of the four-momentum transfer in $pn+$ events, assuming the process of Fig. 12(a). The prediction of Selleri (Ref. 14) is shown for comparison. (a) All $pn+$ events. (b) Events in the isobar peak only.

If the OPEM is extended to the entire physical region, specific predictions of differential cross sections may be made. Selleri[14] has derived an expression for the distribution of neutron kinetic energy in the frame of the incident proton at the upper vertex of Fig. 12(a). The Δ^2 distribution discussed above is equivalent to this distribution. Figure 16(a) compares our results with those calculated from Selleri's equation; Fig. 16(b) shows the same two curves for events in the isobar peak only, where Selleri's predictions should be better since he neglects the process of Fig. 12(b). The over-all shapes agree fairly well, except that the experimental curve ends near $\Delta^2=1.2$ (BeV/c)^2 because of the procedure of choosing the lower Δ^2 for each event. However, Selleri's predictions for the total $pn+$ cross sections, 19.0 and 14.3 mb for Figs. 16(a) and 16(b), respectively, are higher than our results ($17.2_{-0.6}^{+0.7}$ mb and $11.1_{-0.4}^{+0.5}$ mb). One possible explanation of this discrepancy is "absorptive damping" by competing channels.[15]

Another prediction of the OPEM is that the pion-proton scattering angle α in the isobar rest frame should behave like the same angle in real pion-proton scattering. Then for events in the peak, the distribution of events should have the form $1+2.5\cos^2\alpha$, the average

[13] W. O. Lock, *High Energy Nuclear Physics* (John Wiley & Sons, Inc., New York, 1960), Chap. IV.

[14] F. Selleri, Phys. Rev. Letters **6**, 64 (1961).

[15] K. Gottfried and J. D. Jackson, CERN Report 8956/Th. 428 (unpublished).

distribution in the peak for π^+p scattering. The experimental distribution was plotted for events with $\Delta^2<0.16$ (BeV/c)^2. The best fit of the form A $(1+B\cos^2\alpha)$ gives $B\approx0.55$, and is a very poor fit. (χ^2 probability ~0.02.)

Treiman and Yang have proposed another test of the OPEM in the physical region.[16] Pions are spinless; therefore the virtual pion exchange between the vertices of Fig. 12(a) can carry no information correlating the planes of the interactions at the two vertices. The angle between the normals to these planes is called the Treiman-Yang angle, and was calculated in the reference frame (either lab system or rest frame of the beam) in which the collision was more peripheral. Figure 17 shows the distributions of the Treiman-Yang angle for all events, for events with $\Delta^2<0.16$ (BeV/c)^2, and for events with $\Delta^2<0.08$ (BeV/c)^2. [0.08 and 0.16 (BeV/c)^2 correspond approximately to $4m_\pi^2$ and $8m_\pi^2$, respectively.] Figure 18 shows the same three curves for events in the isobar peak only. All the distributions are consistent with isotropy, with χ^2 probabilities between 0.25 and 0.80. As would be expected from the OPEM (because the influence of the one-pion pole is most dominant for low Δ^2), the distributions with $\Delta^2<0.08$ (BeV/c)^2 come closest to isotropy. Actually, as Ferrari has pointed out,[17] interference from the process of Fig. 12(b) leads to a predicted deviation from isotropy of about 10% in the isobar peak and to an even greater deviation outside the peak. However, the statistics of this experiment are not sufficient to detect small deviations from isotropy.

CONCLUSIONS

The principal results of this study of proton-proton interactions at 1.48 BeV are:

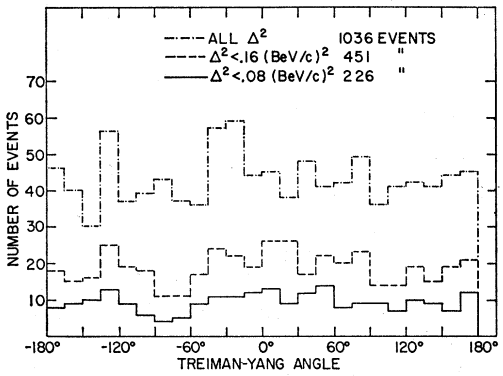

FIG. 17. Distributions of the Treiman-Yang angle for all events in different ranges of the square of the four-momentum transfer, assuming the process of Fig. 12(a).

[16] S. B. Treiman and C. N. Yang, Phys. Rev. Letters 8, 140 (1962).

[17] E. Ferrari, Phys. Letters 2, 66 (1962).

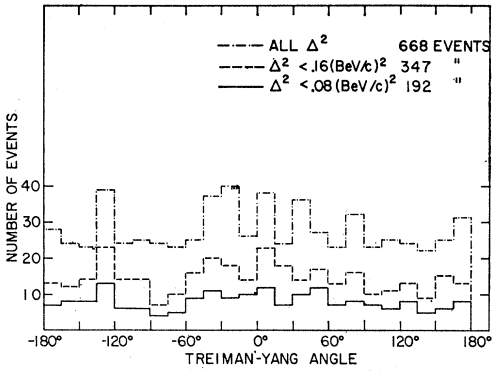

FIG. 18. Distributions of the Treiman-Yang angle for events in the isobar peak only in different ranges of four-momentum transfer squared.

(1) The elastic total cross section is $19.86_{-0.64}{}^{+0.73}$ mb, and the elastic angular distribution fits reasonably well to a simple opaque-disk optical model with parameters $R=0.91$ F and $1-a=0.864$.

(2) The principal pion-production reaction $p+p\rightarrow p+n+\pi^+$ is clearly dominated by $(\frac{3}{2},\frac{3}{2})$ isobar production and is peripheral in nature. The $I=\frac{1}{2}$ isobar appears to contribute little to the reaction, with $\sigma(N_1^*)/\sigma(N_2^*)=7$. However, the decay of the isobar in its own c.m. system does not appear isotropic.

(3) At least three tests of the one-pion-exchange model are satisfied. The Chew-Low extrapolation yields a π^+p cross section averaged over the isobar peak of 127 ± 76 mb, in reasonable agreement both with the measured value and with previous extrapolations at 2.02 and 2.85 BeV. Second, the Treiman-Yang angle is apparently isotropic, as predicted by the OPEM. Finally, the neutron kinetic-energy distribution derived by Selleri, which is based on the OPEM, agrees in shape with the experimental distribution. The total $pn+$ cross section is 10% to 20% lower than that obtained from integrating Selleri's predicted distribution. However, the OPEM prediction that the pion-proton scattering angle in the isobar rest frame should have the form $1+2.5\cos^2\alpha$ is not satisfied.

ACKNOWLEDGMENTS

The authors wish to acknowledge the assistance of the BNL 20-in. bubble-chamber operating crew and that of the staff of the Cosmotron Department. We are also indebted to Dr. D. K. Robinson for his program for obtaining the neutron energy distribution predicted by Selleri, and also for several useful discussions. Finally, we wish to thank our patient scanners and measurers, without whom bubble-chamber experiments would not be possible.